ACS OMEGA

http://pubs.acs.org/journal/acsodf

Article

Electrospun Nanofibers from Waste Polyvinyl Chloride Loaded Silver and Titanium Dioxide for Water Treatment Applications

Akmal Zulfi,* Sri Hartati, Syarifa Nur'aini, Alfian Noviyanto,* and Muhamad Nasir

Cite This: *ACS Omega* 2023, 8, 23622−23632

Read Online

ACCESS | Metrics & More | Article Recommendations

ABSTRACT: The electrospun nanofiber membrane from polyvinyl chloride (PVC) waste for water treatment applications has been successfully produced. The PVC precursor solution was prepared by dissolving the PVC waste in DMAc solvent, and a centrifuge was used to separate undissolved materials from the precursor solution. Ag and TiO_2 were added to the precursor solution before the electrospinning process. We studied the fabricated PVC membranes using SEM, EDS, XRF, XRD, and FTIR to study the fiber and membrane properties. The SEM images depicted that Ag and TiO_2 addition has changed the morphology and size of fibers. The EDS images and XRF spectra confirmed the presence of Ag and TiO_2 on the nanofiber membrane. The XRD spectra showed the amorphous structure of all membranes. The FTIR result indicated that the solvent completely evaporated throughout the spinning process. The fabricated PVC@Ag/TiO_2 nanofiber membrane showed the photocatalytic degradation of dyes under visible light. The filtration test on the membrane PVC and PVC@Ag/TiO_2 depicted that the presence of Ag and TiO_2 affected the flux and separation factor of the membrane.

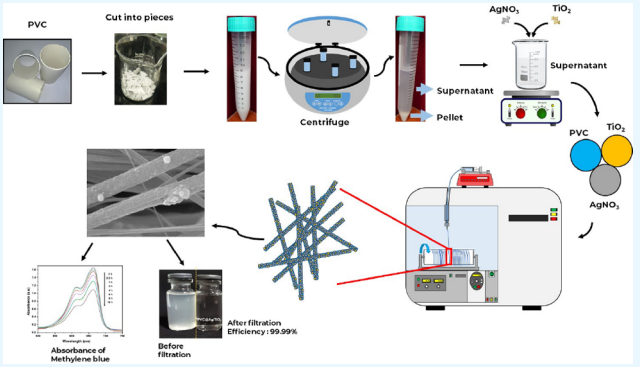

INTRODUCTION

Currently, plastic has become an essential material and is involved in almost all lines of people's life. Many daily goods use plastic as a primary material, such as household furniture, electronics, medical devices, packaging materials, and many more.[1,2] Of all the most used types of plastic, polymer polyvinyl chloride, or "PVC", is one of the most well-known. In 2018, the demand for this type of polymer plastic exceeded 44.3 million tons globally and is expected to increase to nearly 60 million tons by 2025.[3] PVC plastic is currently the second largest volume of polymer plastic after polyethylene in the plastics industry.[4] The extensive use of PVC has caused plastic waste to increase in recent years; suppose that this needs to be offset by better plastic waste processing. In that case, the plastic waste will end up in the ocean and cause damage to the environment.[4] Incineration and landfills are the most straightforward solutions to dealing with plastic waste. However, there are better solutions than this because it will cause new environmental problems, considering that PVC products contain chlorine, which is very dangerous if burned or buried.[4,5] Recycling is a more acceptable route to reduce the accumulation of PVC waste without any environmental problems and, at the same time, reclaim the material content of PVC waste.

Several studies have reported on the recycling process of PVC waste. In a study by Fakhri et al., PVC waste was used as additional material in the asphalt.[6] Then, Merlo et al. used PVC waste as an additional aggregate in light mortar production.[7] Moreover, Manjunatha et al. also studied and compared the environmental impact and energy needs for concrete production, which used PVC waste powder and conventional concrete.[8] Despite the successful report of PVC waste that several researchers have published, the accumulation of PVC waste increases continuously due to increasing PVC production for daily use. Therefore, alternative solutions are highly required to enhance the recycling process of PVC waste. Previous studies have reported using polymeric waste as the nanofiber material. This can be an excellent chance to mitigate PVC waste. Aside from avoiding environmental issues, this option could reduce the material cost of producing nanofiber membranes. Furthermore, the recycling of PVC waste into a nanofiber membrane has not been reported in any literature. It might be because the PVC products such as PVC pipe comprise a variety of additives, leading to complicated

Received: March 10, 2023
Accepted: May 25, 2023
Published: June 21, 2023

https://doi.org/10.1021/acsomega.3c01632
ACS Omega 2023, 8, 23622−23632

processing in electrospinning and with inferior physical and mechanical properties of the resulting membrane. So to produce a better product, separation of the PVC polymer and its additive material is needed.[4,9]

Nanofiber membranes have high porosity and interconnected and tortuous pore structures, providing high selectivity and permeability in water filtration.[10,11] Chen et al. (2022) reported that the PAN/TPU nanofiber membrane had a retention efficiency of up to 99.99% for 100 nm of SiO_2 suspension with a high pure water flux of ~8490 L m^{-2} h^{-1}.[12] In addition, a nanofiber membrane also has a good ability to separate oil and water.[13,14] Recently, a nanofiber membrane with photocatalytic activity has also attracted much attention. For example, Wang et al. (2020) reported that the PAN/Ag/TiO_2 nanofiber membrane has high photodegradation efficiency for methylene blue, rhodamine B, and methyl orange.[15] Then, Kanjwal et al. (2016) successfully fabricated the hybrid matrices of the TiO_2-Ag nanofiber with silicone as the photocatalyst to degrade dairy wastewater.[16] It would be interesting to develop a membrane from PVC waste with photocatalytic performance and high efficiency of particles.

Electrospinning is one of the methods of fabricating a nanofiber-based membrane, which consists of any main components such as a high-voltage (HV) source, a syringe with a metal needle, a syringe pump, and a collector.[17] This method uses a high electric field to fabricate a nanofiber from the polymeric solution. The morphology and size of the nanofiber can be controlled by adjusting the parameters of solution (such as surface tension, viscosity, and conductivity), processing (such as applied voltage, the distance of the needle tip to a collector, and solution flow rate), and environmental (such as humidity).[18,19]

The PVC pure polymer as a composite nanofiber has been studied for various studies including applications for the methanol microsensor,[20] terahertz optical component,[21] heavy metal removal,[22] etc. To our knowledge, the PVC waste is rarely studied as the nanofiber area. This is the first study that discusses the PVC waste recycling process with the electrospinning method into the nanofiber membrane and becomes suitable for water treatment applications. The precursor solution was prepared by dissolving PVC waste with DMAc solvent. Then, a centrifuge was used to separate undissolved materials from the precursor solution. The addition of Ag and TiO_2 in the precursor solution was produced to get the photocatalytic activity of the fabricated nanofiber membrane. The effect of adding Ag and TiO_2 on the diameter, morphology, composition, crystallinity, and functional groups of fabricated nanofiber membranes was studied. The photocatalytic activity of fabricated nanofiber membranes was also studied by perceiving the degradation of dyes. We also examined the ability of the fabricated nanofiber membranes to capture antacid particles of ~850 nm in size.

RESULTS AND DISCUSSION

Characterization of Nanofiber Membranes. Figure 1 shows the SEM images and size distribution of electrospun PVC and PVC@Ag/TiO_2 nanofiber membranes.

Figure 1a shows the morphology and size distribution of the PVC nanofiber membrane, which has an average diameter of around 0.58 μm. In addition, the morphology of the nanofiber membrane became more variated after mixing with Ag and TiO_2, as seen in Figure 1b. The average fiber diameter decreased to 0.37 μm, and the fiber morphology remained

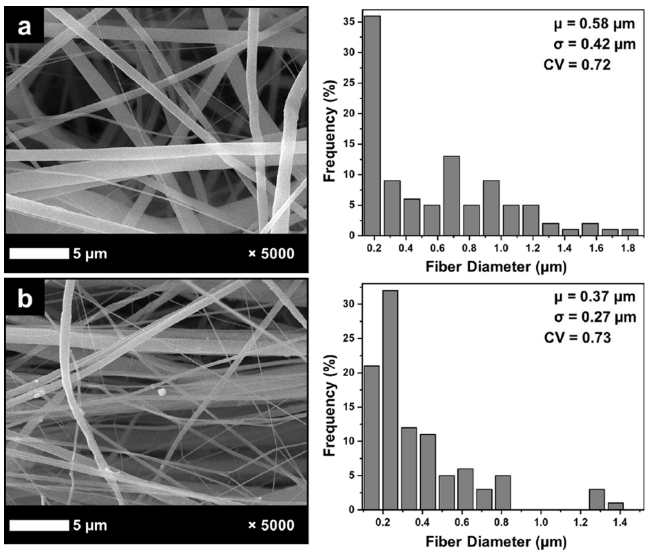

Figure 1. SEM image of the (a) PVC nanofiber membrane and (b) PVC@Ag/TiO_2 nanofiber membrane.

without beads. The histograms show that the nanofiber membranes PVC and PVC@Ag/TiO_2 had CV above 0.3, so they were categorized as nonuniform nanofibers.[19] Reduction of the average fiber diameter may be due to the presence of Ag, which has been reported by several studies. They described that the higher Ag in nanofiber TiO_2 leads to a reduction of the fiber diameter.[23,24] It can be explained by the fact that the conductivity of a solution with the addition of $AgNO_3$ is higher compared to a solution without $AgNO_3$, allowing a higher surface charge of the polymer jet and facilitating a better elongation of the fiber by the applied electric field.[25] Ag and TiO_2 contributed to increasing the roughness of the nanofiber surface, as shown in Figure 1b. Similar results regarding Ag and TiO_2 on the surface of the nanofiber were also reported by previous studies.[26−28] The SEM image of the PVC@Ag/TiO_2 nanofiber membrane magnified 30,000 times was included for better observation in Figure 2.

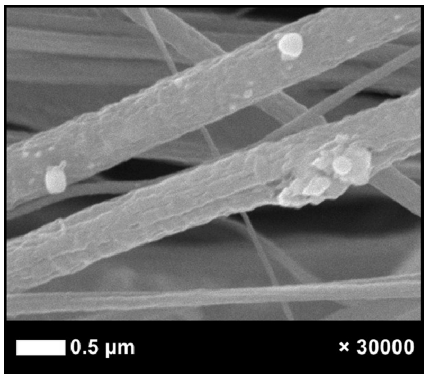

Figure 2. SEM images of PVC@Ag/TiO_2 nanofiber membranes.

Figure 3 displays the XRF spectra of PVC and PVC@Ag/TiO_2 nanofiber membranes in mid-Z and high-Z ranges. The spectrum in Figure 3a confirms the presence of Ti, including Ti-K_α (4.51 keV) and Ti-K_β (4.94 keV), on the PVC@Ag/TiO_2 nanofiber membrane.[29,30] Then, Figure 3b shows the presence of Ag on the PVC/Ag/TiO_2 nanofiber membrane with peaks of 22.19 and 25.02 keV for Ag-K_α and Ag-K_β,

https://doi.org/10.1021/acsomega.3c01632
ACS Omega 2023, 8, 23622−23632

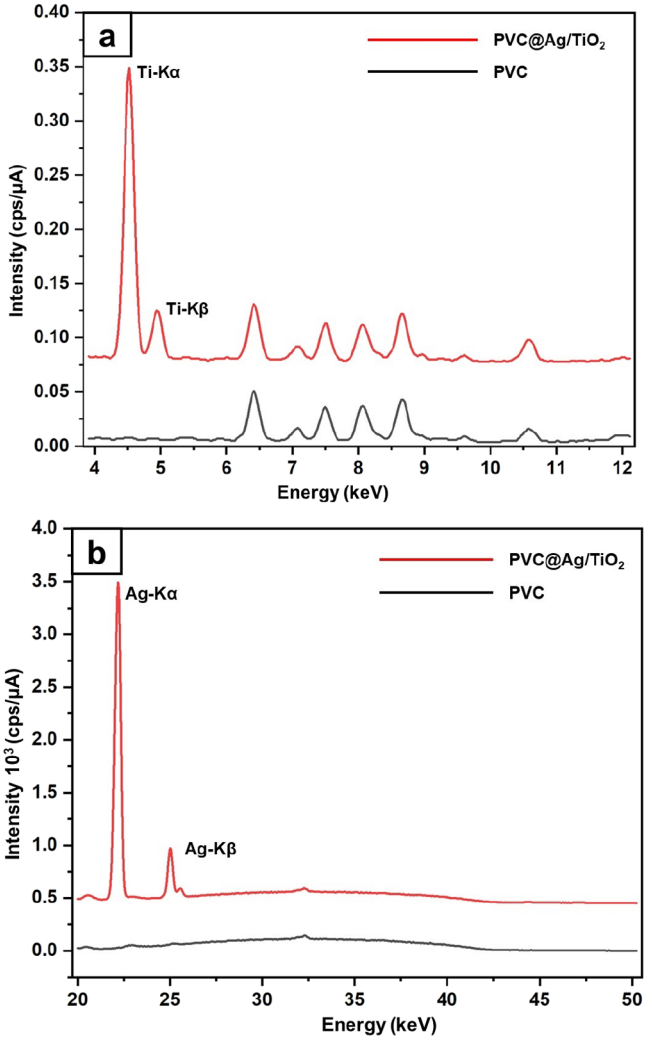

Figure 3. XRF images of PVC and PVC@Ag/TiO_2 nanofiber membranes operating in the (a) mid-*Z* range (4 to 12 keV) and (b) high-*Z* range (20 to 50 keV).

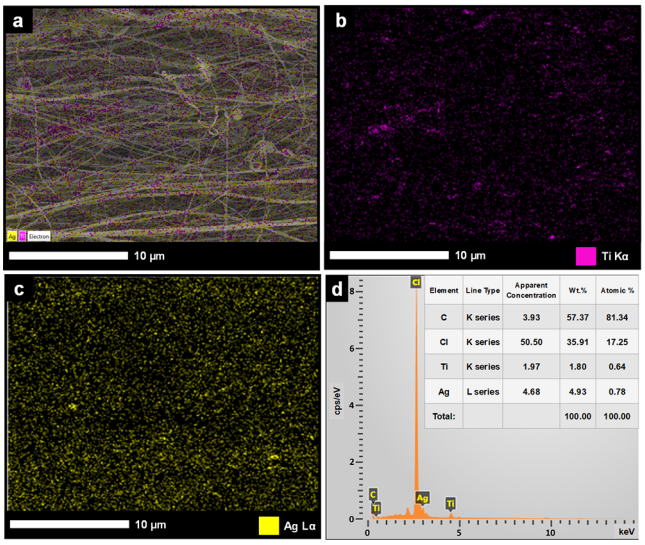

Figure 4. SEM images of PVC@Ag/TiO_2 (a) EDX mapping of the area containing Ag and Ti in the nanofiber membrane; (b) EDX mapping of the area containing Ti; (c) EDX mapping of the area containing Ag; and (d) EDX spectrum.

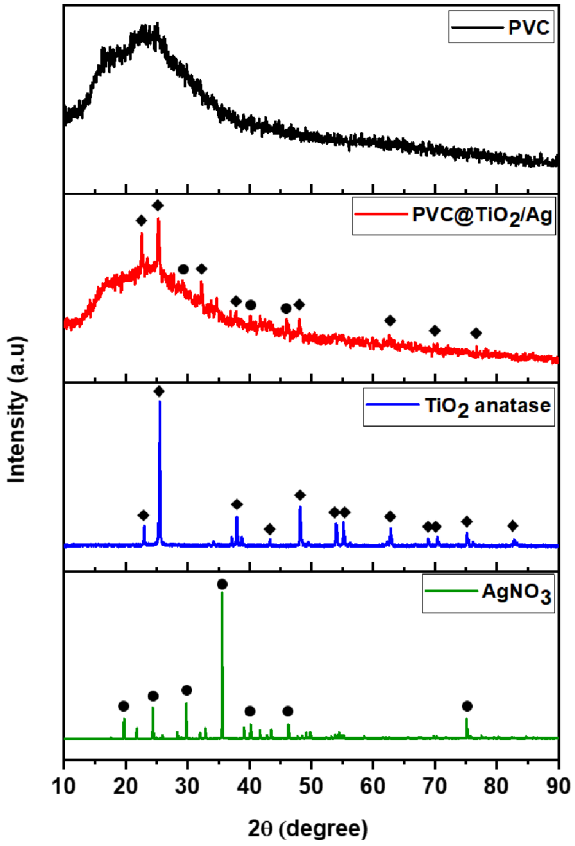

Figure 5. X-ray diffractograms of the PVC nanofiber membrane, PVC@Ag/TiO_2 nanofiber membrane, TiO_2, and $AgNO_3$.

respectively.[31,32] Meanwhile, the PVC nanofiber membrane did not show Ag or TiO_2 peaks. Furthermore, PVC and PVC/Ag/TiO_2 nanofiber membranes were not affected by the other elements, indicating that the Ag and TiO_2 are compositionally pure.

Figure 4a shows the morphology of a PVC@Ag/TiO_2 nanofiber membrane containing Ag and TiO_2. The elemental mapping of Ti and Ag is depicted in Figure 4b,c, respectively. Ag and Ti were uniformly distributed throughout the PVC@Ag/TiO_2 nanofiber membrane. The quantity of membrane elements is presented in Figure 4d. The Cl element has a concentration of 57.37 wt %, followed by C, Ag, and Ti, with concentrations of 35.91, 4.93, and 1.97 wt %, respectively. It is reasonable for the high concentration of Cl and C elements since they are PVC's main components.[33,34] Furthermore, the Ag concentration was higher than Ti due to the amount of Ag being higher than Ti in the precursor solution. Similar results have been reported by Lubasova and Barbora (2014).[35]

Figure 5 shows the XRD patterns of the PVC, PVC@Ag/TiO_2 nanofiber membranes, TiO_2 anatase, and $AgNO_3$. Several studies have reported that pure PVC has a broad peak that indicates the amorphous nature of PVC in the 2θ region of ~12 to ~35°.[36,37] This was suitable with our XRD result from the PVC nanofiber membrane. In general, an electrospun nanofiber membrane does have an amorphous structure. It was due to the Coulombic force in the spinning process. The polymer solution was pulled to the collector, solvent evaporation occurred very fast, and the crystallization process was not appropriately proceeded, leading to an amorphous structure formation.[38]

https://doi.org/10.1021/acsomega.3c01632
ACS Omega 2023, 8, 23622−23632

Meanwhile, the XRD pattern of the PVC@Ag/TiO_2 nanofiber membrane shows new diffraction peaks after mixing with Ag and TiO_2. The patterns of crystal structures of TiO_2 are represented by a diamond sign in Figure 5. We used anatase TiO_2, and then it was confirmed as the anatase structure with the highest diffraction peak at 25.4°.[39] Based on JCPDS card number 12-1272, the peak patterns of anatase TiO_2 are at 25.4, 37.9, 47.9, and 62.9°, which correspond to the (101), (103), (200), and (204) crystal planes, respectively.[40,41] Most of the TiO_2 peaks appear in the PVC@Ag/TiO_2 nanofiber membrane. However, the TiO_2 peak on 2θ 22.88° is shifting slightly to 22.53° on the PVC@Ag/TiO_2 nanofiber membrane. The anatase TiO_2 was chosen because it has higher photocatalytic activity than rutile TiO_2.[42]

On the other side, crystal structures of $AgNO_3$ are represented by spherical signs in Figure 5. Peaks at 27.8, 32.1, and 38.1° belong to the Ag crystal corresponding to the (210), (122), and (111) crystal planes, respectively.[43] The peaks of Ag in the PVC@Ag/TiO_2 nanofiber membrane only appear in a very low intensity. It might be due to the silver nanoparticles being finely dispersed in the precursor solution, and after deposition in the nanofiber, the Ag crystal is not formed properly.[44] In conclusion, the crystallinity of Ag and TiO_2 decreased after deposition on the PVC nanofiber, which is indicated by the low peak intensity of Ag and TiO_2 in the PVC@Ag/TiO_2 nanofiber membrane.

Figure 6 shows the absorbance band characteristics of the PVC and PVC@Ag/TiO_2 nanofiber membranes. There was

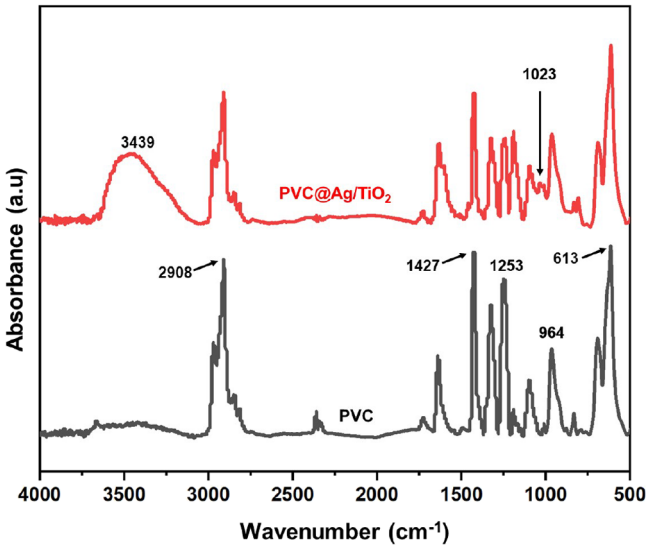

Figure 6. FTIR spectra of the PVC and PVC@Ag/TiO_2 nanofiber membranes.

absorbance at 2908 cm^{-1} (assigned to C−H stretching), 1427 cm^{-1} (assigned to CH_2 deformation), 1253 cm^{-1} (assigned to CH−rocking), 964 cm^{-1} (assigned to *trans* CH wagging), and 613 cm^{-1} (assigned to C−Cl stretching), which were the characteristics of the PVC polymer.[45,46] After adding Ag and TiO_2, a broad peak appeared at ∼3439 cm^{-1}, assigned to the stretching vibration of the hydroxyl group (−OH). It is due to the water molecules and CO_2 absorption from the air.[40] This peak also corresponds to the O−H stretch region, which is attributed to the interaction between the hydroxyl groups of titania.[47] Then, a new peak also appeared at 1023 cm^{-1}, related to the stretching vibration of Ti−O−C bonding.[48]

The peaks of DMAc solvent (at 1011, 1392, 1633, and 2931 cm^{-1}) did not appear on the FTIR spectra of the fabricated PVC or PVC@Ag/TiO_2 nanofiber membranes.[49,50] The fabricated PVC nanofiber membrane also had a high similarity of peaks with a nanofiber made from pure PVC reported by Quoc et al. (2021).[45] It indicates that the DMAc solvents entirely evaporated during the electrospinning process. Overall, these results (SEM, EDS, XRF, XRD, and FTIR) indicate that the centrifuge process allows the separation of the PVC polymer from additives of the PVC pipe.

Photocatalytic Activity. Degradation of different dye solutions was conducted to investigate the photocatalytic activity of the PVC@Ag/TiO_2 nanofiber membrane. Figure 7

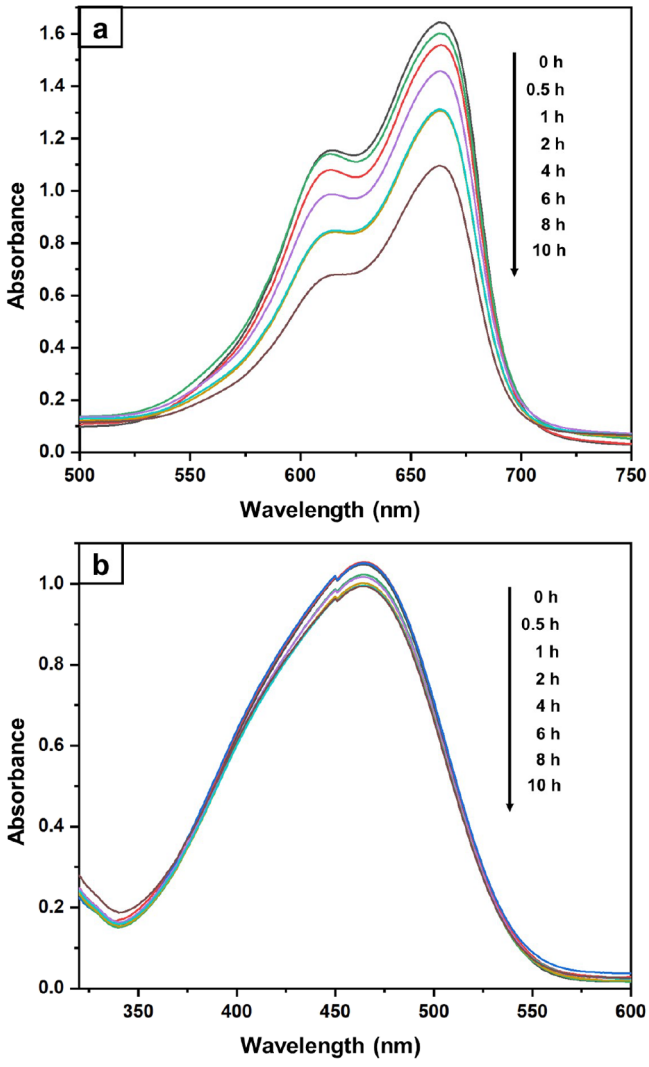

Figure 7. Absorbance of (a) methylene blue and (b) methyl orange for various irradiation times of the PVC@Ag/TiO_2 nanofiber membrane.

shows the change in the optical absorption spectra of methylene blue and methyl orange by the PVC@Ag/TiO_2 nanofiber membrane under visible light irradiation for different time intervals. The photocatalytic process depends on the interaction between a light source and the surface of materials, with two or more reactions co-occurring during the process.

https://doi.org/10.1021/acsomega.3c01632
ACS Omega 2023, 8, 23622−23632

There is an oxidation reaction to help the photogeneration of holes and a reduction reaction to support the photogeneration of electrons.[51] The process will conduct efficiently if the optical band gap energy is low since the electron from the conduction band will easily be generated to promote the photocatalytic process. It means that the exposure of light with a specific wavelength and materials influences the photocatalytic process.[52] Previous studies reported that nanofibers with the addition of TiO_2 and Ag had excellent photocatalytic activity under visible light.[15,26]

As shown in Figure 7a, the photocatalytic degradation rates of the methylene blue in the presence of PVC@Ag/TiO_2 decreased if the immersion time was longer. This result showed that the PVC@Ag/TiO_2 nanofiber membrane has photocatalytic activity under visible light. In general, a TiO_2 photocatalyst is in the UV region.[53] The presence of Ag in the PVC@Ag/TiO_2 nanofiber membrane can enhance the interfacial charge transfer and electron−hole separation in the PVC@Ag/TiO_2 nanofiber membrane, improving the photocatalytic activity and working area of TiO_2 to the visible light region.[54,55] Wang et al. (2020) and Hartati et al. (2022) also reported a similar photocatalytic activity for the PAN nanofiber membrane loaded with TiO_2 and Ag. Figure 7b shows the absorbance of methyl orange for various irradiation times in the presence of the PVC@Ag/TiO_2 nanofiber membrane.[15,26] Based on Figure 7b, the absorbance spectrum of methyl orange was almost similar, which means that the PVC@Ag/TiO_2 nanofiber membrane was not optimum for degraded methyl orange. Several studies reported that the degradation of dye solutions, including methylene blue, methyl orange, and rhodamine B, on the nanofiber membrane loaded with TiO_2 and Ag was different for each.[15,26,56] This indicates that pollutants' properties and chemical structure influence the photocatalytic activity of the PVC@Ag/TiO_2 nanofiber membrane.

Water Filtration Test. The pure water flux of PVC and PVC@Ag/TiO_2 nanofiber membranes was tested with increasing pressure, and the results are shown in Figure 8. Based on the flux−pressure curves, all nanofiber membranes show linear dependencies of the flux to the pressure and it is corresponding to Darcy's law.[57] The flux of nanofiber membranes can be affected by several factors, including hydrophilicity, fiber diameter, and membrane thickness.[58,59]

Fauzi et al. (2020)[57] have reported reducing nanofiber membranes' flux due to decreasing fiber diameter. The smaller fiber diameter yields a smaller membrane pore size, making it harder for water to pass through the membrane.[58,60,61] Contrarily, the PVC@Ag/TiO_2 nanofiber membrane (μ of 0.37 μm) had a higher flux than that of the PVC nanofiber membrane (μ of 0.58 μm), even though the PVC nanofiber membrane had the larger fiber diameter. This condition might be related to Ag and TiO_2 presence in the nanofiber membrane. Hartati et al. (2022) reported that the presence of Ag and TiO_2 in a PAN nanofiber membrane changes the wettability of the PAN membrane from hydrophobic to hydrophilic.[26] In water filtration, increasing membrane hydrophilicity will lower the capillary pressure of filter media and enhance the water flow rate.[62]

Figure 9a shows the plot of the pure water flux as a function of time at an applied pressure of 0.05 bar from PVC and PVC@Ag/TiO_2 nanofiber membranes. It was seen that throughout the 30 min test period, the pure water fluxes of all membranes were still relatively constant. Liu et al. (2013)

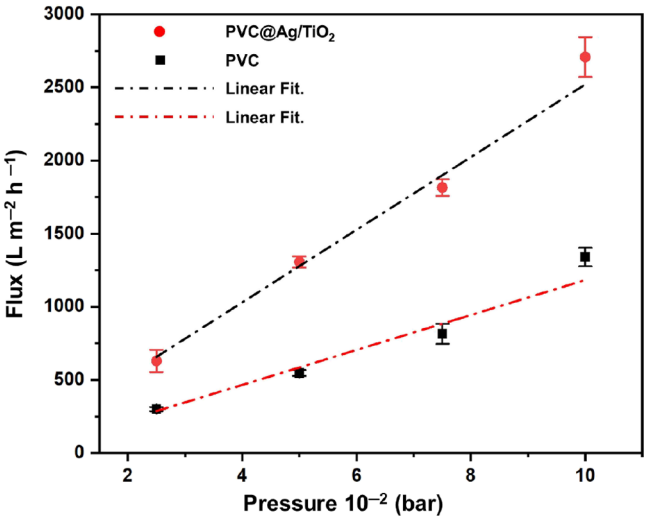

Figure 8. Pressure and pure water flux relations for PVC and PVC@Ag/TiO_2 nanofiber membranes.

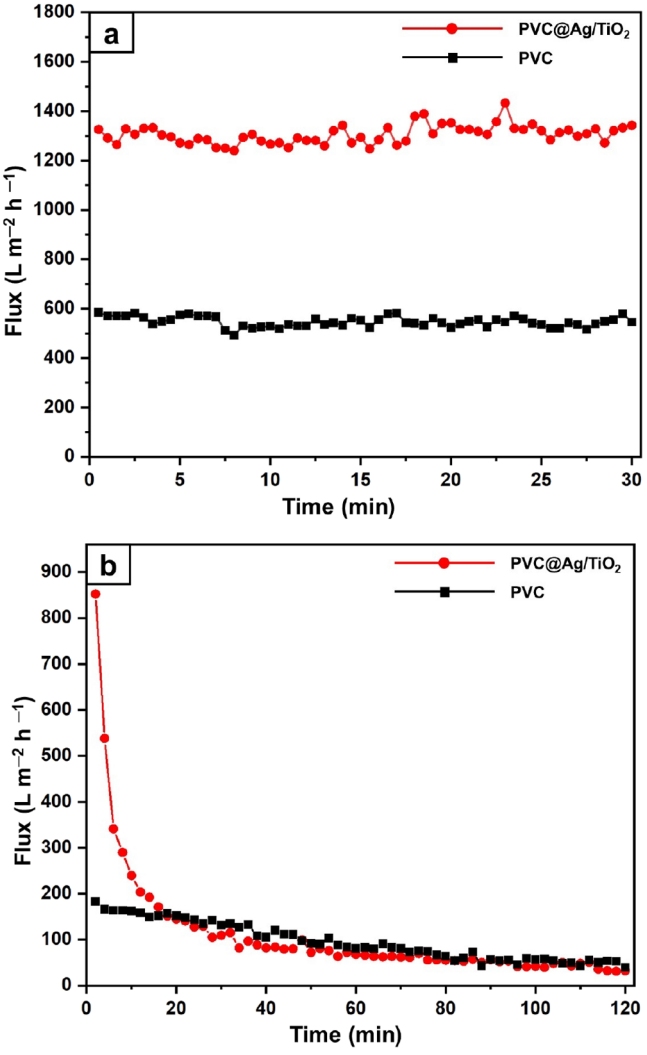

Figure 9. Time dependence of the (a) pure water flux and (b) permeate flux in the rejection tests for PVC and PVC@Ag/TiO_2 nanofiber membranes under an applied pressure of 0.05 bar.

https://doi.org/10.1021/acsomega.3c01632
ACS Omega 2023, 8, 23622−23632

also reported similar trends of pure water flux as a function of time for electrospun PVA nanofiber membranes.[59]

Figure 9b depicts the flux change of PVC and PVC@Ag/TiO_2 nanofiber membranes during a rejection test, a test period of 120 min with flux measurement every 2 min. Based on Figure 9b, the PVC@Ag/TiO_2 nanofiber membrane exhibited the highest initial flux, in line with the results obtained previously (Figures 8 and 9a). In the beginning, the permeate flux dropped very quickly, and after 40 min of the rejection test, the change was more stable. Similarly, the permeate flux of the PVC nanofiber membrane also dropped quickly. In dead-end filtration, the particles easily collect on the nanofiber membrane's top surface and form a "cake layer", reducing the pore size and decreasing the permeability of the nanofiber membrane with time. Because of that, the flux reduces sharply along the rejection test (Figure 10).[57,59,63]

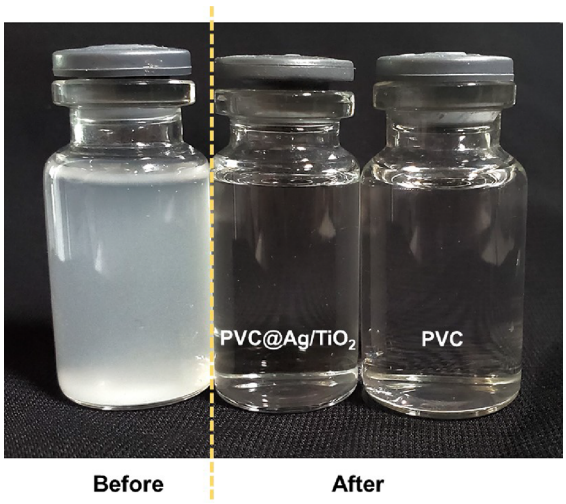

Figure 10. Visual illustration of the antacid solution prepared before and after the filtration test. (Photograph courtesy of Syarifa Nur'aini. Copyright 2022.)

As shown in Table 1, the PVC@Ag/TiO_2 nanofiber membrane had slightly better performance than the PVC nanofiber membrane, and the explanation is as follows. Compared with the PVC nanofiber membrane, the PVC@Ag/TiO_2 nanofiber membrane had a smaller average fiber diameter. As previously discussed, the diameter of the fiber directly impacts the pore size, in which the smaller fiber diameter forms the smaller pores. Smaller pores hardly allowed the particle to pass through the nanofiber membranes.[57,64] All results indicated the promising application of the PVC@Ag/TiO_2 nanofiber membrane as water filtration media. Furthermore, we also compared our study with other articles shown in Table 2. Based on Table 2, our membrane has a better performance than several previously reported studies. These results were quite satisfactory, considering that the waste PVC materials could compete with pure polymer materials.

Table 1. Separation Factor of PVC and PVC@Ag/TiO_2 Nanofiber Membranes for Antacid Particles

sample name	PVC	PVC@Ag/TiO_2
SF (%)	99.98	99.99

Table 2. Other Studies about the Nanofiber and Composite for Water Filtration

precursor	fiber diameter (nm)	flux (L m^{-2} h^{-1})	efficiency (%)
PVA/TEOS[66]	~500		
PAN/PVDF[67]	~300	1000−1200	40−80
RSNF[68]	~4−~7	~200−600	99
CA/chitin[69]	500−1700	27,900	
PMIA[70]	~500−~700	259	94.7
PSU[71]	690−830	99−8590	95.9
PES[72]	550−1300	160	100
PAN[64]	100−500	118	99
PVA/TiO_2[73]	319−360	7500−13,500	99
PVC@Ag/TiO_2 (this study)	~370	~1300	99.99

CONCLUSIONS

Nanofiber-based membranes made from PVC waste as water filtration media have been successfully produced using the electrospinning method. PVC nanofiber membranes were made with and without the addition of Ag and TiO_2. The addition of Ag and TiO_2 caused a decrease in the average fiber diameter. Ag and TiO_2 were well distributed in the fabricated nanofiber membrane in which the presence and composition were proved by XRF and EDS. Peaks of Ag and TiO_2 were still observed in the PVC@Ag/TiO_2 nanofiber membrane, while the XRD result showed an amorphous structure. Based on the FTIR spectra, all the solvents entirely evaporated along the electrospinning process. Overall, the nanofiber membrane from PVC waste successfully loaded Ag and TiO_2, and the centrifuge process separated the PVC polymer from additives of the PVC pipe. Perhaps, this process could be applied in the chemical recycling of other plastic kinds. The photocatalytic activity of PVC@Ag/TiO_2 nanofiber membranes was proved by the degradation of the dye's solution under visible light. We performed a filtration test on fabricated membranes with particles ~850 nm in size. The test results depicted that the PVC@Ag/TiO_2 nanofiber membrane had a higher flux and separation factor (99.99%). The smaller average fiber size of the PVC@Ag/TiO_2 nanofiber membrane can effectively capture the particle, leading to high rejection. These results can promote the opportunity of PVC waste as a nanofiber membrane for water treatment applications.

EXPERIMENTAL SECTION

Materials. The waste of the PVC pipe (Ganesha, Indonesia) was collected as the PVC material. TiO_2 anatase and *N*,*N*-dimethylacetamide (DMAc) solvent were purchased from Sigma-Aldrich, Singapore. Then, $AgNO_3$ (Merck, Germany) was purchased from a local supplier. In addition, commercial nonwoven polyethylene terephthalate was used as a membrane substrate. Figure 11 shows the PVC waste that was used during the research.

Precursor Solution. The preparation of the precursor solution started with washing PVC waste with water and drying it at room temperature. Then, the PVC waste was cut into small pieces and dissolved in DMAc solvent. The solution was stirred for ~16 h at room temperature until it turned into a homogeneous solution. Then, the solution was transferred into a centrifugal tube and centrifuged at 3000 rpm for an hour. The used centrifuge was from Biosan, LMC-3000. As most PVC pipe was fabricated with calcium carbonate as a filler, the

https://doi.org/10.1021/acsomega.3c01632
ACS Omega 2023, 8, 23622−23632

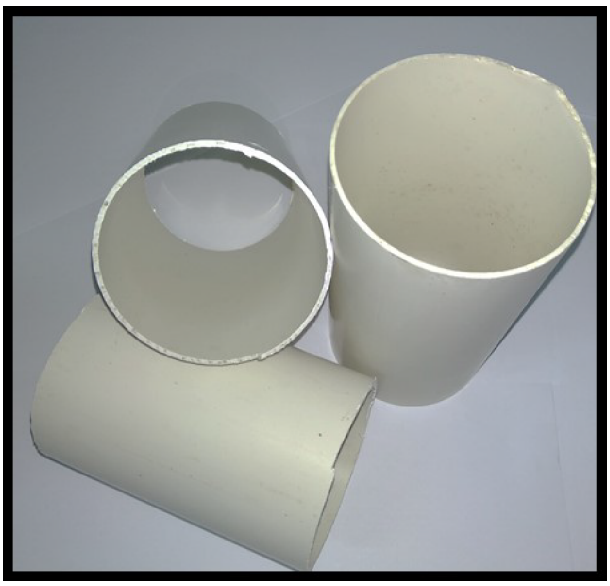

Figure 11. PVC pipe. (Photograph courtesy of Akmal Zulfi. Copyright 2022.)

separation was needed because of the high content of the filler.[74]

The separation also aims to eliminate the waste PVC from other undissolved impurities that might influence the morphology of the membrane. It could be one of the steps to be applied in utilizing the polymeric waste for nanofiber materials. The clarity of the solution can be observed obviously in Figure 12; the pellets as undissolved particles could also be

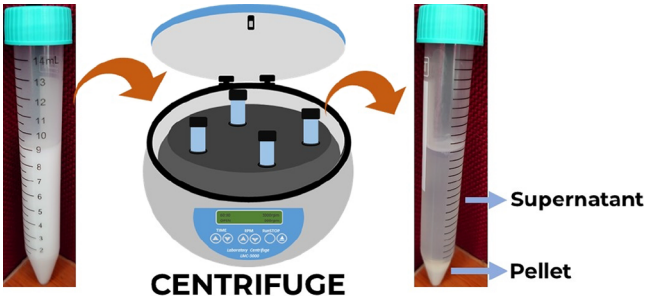

Figure 12. Precursor solution preparation. (Photograph courtesy of Akmal Zulfi. Copyright 2022.)

seen. Then, the supernatant was separated from the pellet and added $AgNO_3$ and TiO_2. Finally, the mixture was stirred for ~24 h at 50 °C. Table 3 shows the variation of the addition of $AgNO_3$ and TiO_2.

Synthesis of Nanofiber Membranes. PVC or PVC@Ag/TiO_2 nanofiber membranes were made using electrospinning (Zuheros Nano, 1.1 M). Figure 13 shows the electrospinning apparatus, which consists of a syringe pump, a rotary drum collector, a rotary drum collector controller, and an HV power supply.

Table 3. Variation of the PVC Solution

sample name	concentration (wt %)	addition of $AgNO_3$ (wt %)	addition of TiO_2 (wt %)
PVC	20	0	0
PVC@Ag/TiO_2	20	2	0.5

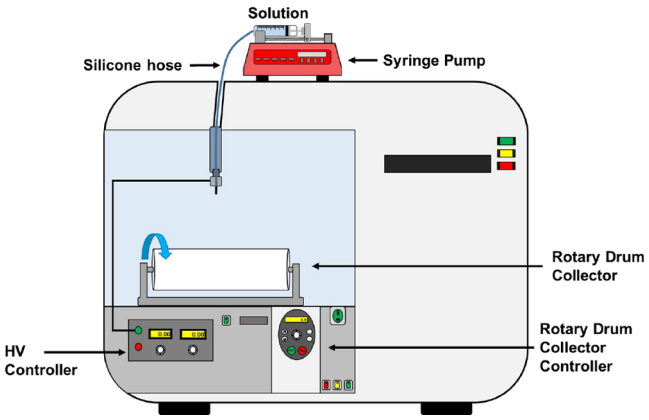

Figure 13. Schematic diagram of electrospinning.

The prepared precursor solution was put into an 8 mL syringe, and then the filled syringe was installed on the syringe pump to control the flow rate of the ejected solution. The syringe was connected to a stainless-steel needle (a needle diameter of 0.7 mm) with a silicone hose. The rotary drum collector was grounded, while the needle was connected to the HV source. The fabricated nanofibers were deposited on a nonwoven fiber membrane wrapping the rotary drum collector. The parameters during the electrospinning process are 25 kV for applied voltage, drum collector to a stainless-steel needle tip distance of 15 cm, a flow rate of solution of 0.1 mL/h, and a humidity of ~50%, which were kept constant.

Characterization of Nanofiber Membranes. The size and morphology of PVC or PVC@Ag/TiO_2 nanofibers were observed using a scanning electron microscope (SEM, JEOL, JSM IT300) with 5000 and 30,000 times magnification. The average fiber diameters and size distributions were determined randomly by measuring the diameter of 100 fibers. The coefficient of variation (CV) was used to define the fiber uniformity, as given in eq 1:

$$\mathrm{CV} = \frac{\sigma}{\mu} \tag{1}$$

where σ is the standard deviation and μ is the average fiber diameter.[75] X-ray fluorescence (XRF, Rigaku NEX OC+ EZ series number QC1520) was used to confirm the presence of Ag and TiO_2 at operating ranges of 4 to 15 and 20 to 50 keV. The distribution of Ag and TiO_2 and their concentration were detected by an EDX detector. The X-ray diffraction patterns of nanofiber membranes were recorded using an X-ray diffractometer (XRD, Rigaku MiniFlex 600), and the diffraction pattern was recorded at a 2θ position in the range of 10 to 90°. The Fourier transform infrared (FTIR) spectra from PVC or PVC@Ag/TiO_2 nanofiber membranes were obtained using an FTIR spectrometer (Thermo Fisher Scientific NICOLET IS10 FTIR spectrometer). The FTIR measurements were done in the wavenumber range of 500−4000 cm^{-1}.

Photocatalytic Activity. The photocatalytic activity of the fabricated nanofiber membrane was studied by perceiving the degradation of the dye's solution under visible light. We used methylene blue and methylene orange as the dye solution. The fabricated nanofiber membrane of 10 mg was put into a 100 mL dye solution with a concentration of 10 ppm. Then, the

https://doi.org/10.1021/acsomega.3c01632
ACS Omega 2023, 8, 23622−23632

dye solution was placed under visible light to allow a photocatalytic reaction. Concentrations of dyes were measured from the UV−vis spectra at different times, while the UV−vis spectra used double-beam UV−vis spectrometry (Labtron LUS-B13 series number M18P210902010).

Water Filtration Performance. A dead-end filtration method equipped with an airflow rate control was used to study the water filtration performance of the fabricated nanofiber membranes. Figure 14 depicts the schematic diagram

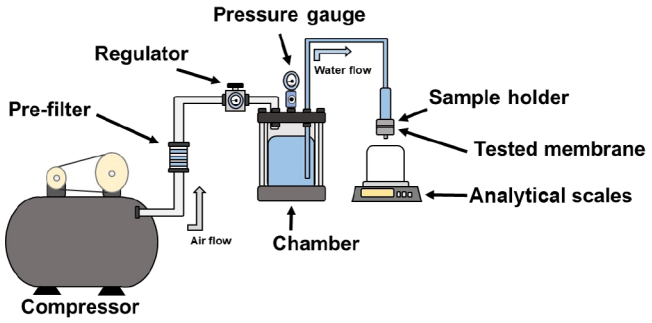

Figure 14. Schematic diagram of the water filter test system.

of the water filter test system. The system consisted of a compressor, a pre-filter, a regulator, a chamber, a pressure gauge, a sample holder, and analytical scales. The compressor, pre-filter, and regulator provide a clean and stable airflow to the chamber. The airflow from the compressor pushed the water out of the chamber to the sample holder. The pressure gauge measured the pressure of the air in the chamber. The tested membrane was placed inside the sample holder. The water passed through the tested membrane, while the analytical scales measured the water out of the sample holder. The tested membrane had a disc shape with a diameter of 25 mm and an electrospinning duration of 2 h.

In this study, the water filtration performance was obtained by measuring the flux of pure water, removal percentage of particles, and separation flux of particles. First, pure water's flux was determined, followed by separating antacid particles (Mylanta, USA).[65] Figure 15 shows the distribution graph of the antacid particle size measured using a particle size analyzer (Beckman Coulter, Delsa Nano C). Antacid particles of 852.1 nm in size were reconstituted in distilled water to prepare a

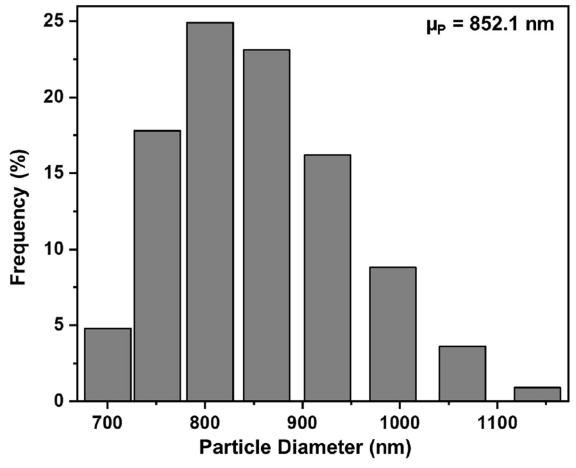

Figure 15. Distribution graph of the antacid particle size.

2500 ppm solution. A calibration curve of the concentration against absorbance was obtained using double-beam UV−vis spectrophotometry (Labtron LUS-B13 series number M18P210902010).

The water flux (J) was determined using eq 2:

$$J = \frac{V}{A.\ \Delta t} \tag{2}$$

where V is the permeate volume, A is the effective membrane area, and Δt is the permeation time.[59]

The double-beam UV−visible spectrophotometer was used to detect the presence of any antacid particles in the permeate, and the calibration curve was used to determine the concentration. The separation factor (SF) was calculated by eq 3:

$$\mathrm{SF} = 1 - \frac{C_{\mathrm{permeate}}}{C_{\mathrm{feed}}} \times 100\% \tag{3}$$

where C_{permeate} is the antacid concentration in the permeate and C_{feed} is the initial antacid concentration in the feed.[63]

■ ASSOCIATED CONTENT

Data Availability Statement

The authors confirm that the data supporting the findings of this study are available within the article [and/or] its Supporting Information.

■ AUTHOR INFORMATION

Corresponding Authors

Akmal Zulfi − *Research Center for Environmental and Clean Technology, National Research and Innovation Agency (BRIN), Bandung 40135, Indonesia;* orcid.org/0000-0001-7075-5386; Email: akmal.zulfi.m@brin.go.id

Alfian Noviyanto − *Nano Center Indonesia, Jalan Raya PUSPIPTEK, South Tangerang, Banten 15314, Indonesia; Department of Mechanical Engineering, Mercu Buana University, Jakarta 11650, Indonesia;* orcid.org/0000-0002-6371-6765; Email: a.noviyanto@nano.or.id

Authors

Sri Hartati − *Nano Center Indonesia, Jalan Raya PUSPIPTEK, South Tangerang, Banten 15314, Indonesia;* orcid.org/0000-0002-6448-8733

Syarifa Nur'aini − *Nano Center Indonesia, Jalan Raya PUSPIPTEK, South Tangerang, Banten 15314, Indonesia*

Muhamad Nasir − *Research Center for Environmental and Clean Technology, National Research and Innovation Agency (BRIN), Bandung 40135, Indonesia*

Complete contact information is available at: https://pubs.acs.org/10.1021/acsomega.3c01632

Author Contributions

A.Z.: conceptualization, methodology, data collection, formal analysis, writing-original draft, and visualization. S.H.: data collection and review-editing. S.N.: data collection and review-editing. A.N.: review and funding acquisition. M.N.: resources and supervision.

Funding

Part of this work was supported by government funding through DIPA of Research Organization of Nanotechnology and Materials (ORNM) Budgetary Year 2023.

https://doi.org/10.1021/acsomega.3c01632
ACS Omega 2023, 8, 23622−23632

Notes

The authors declare no competing financial interest.

■ ACKNOWLEDGMENTS

The authors would like to express their gratitude to Nano Center Indonesia and ELSA BRIN for the facilities and characterization.

■ REFERENCES

(1) Luciani, V.; Bonifazi, G.; Rem, P.; Serranti, S. Upgrading of PVC Rich Wastes by Magnetic Density Separation and Hyperspectral Imaging Quality Control. *Waste Manage.* **2015**, *45*, 118−125.
(2) Pivnenko, K.; Eriksen, M. K.; Martín-Fernández, J. A.; Eriksson, E.; Astrup, T. F. Recycling of Plastic Waste: Presence of Phthalates in Plastics from Households and Industry. *Waste Manage.* **2016**, *54*, 44−52.
(3) Olekhnovich, R. O. A Review on Electrospun PVC Nanofibers: Fabrication, Properties, and Application. *Fibers* **2021**, *9*, 12.
(4) Sadat-Shojai, M.; Bakhshandeh, G. R. Recycling of PVC Wastes. *Polym. Degrad. Stab.* **2011**, *96*, 404−415.
(5) Qiao, W. M.; Yoon, S. H.; Mochida, I.; Yang, J. H. Waste Polyvinylchloride Derived Pitch as a Precursor to Develop Carbon Fibers and Activated Carbon Fibers. *Waste Manage.* **2007**, *27*, 1884−1890.
(6) Fakhri, M.; Shahryari, E.; Ahmadi, T. Investigate the Use of Recycled Polyvinyl Chloride (PVC) Particles in Improving the Mechanical Properties of Stone Mastic Asphalt (SMA). *Constr. Build. Mater.* **2022**, No. 126780.
(7) Merlo, A.; Lavagna, L.; Suarez-Riera, D.; Pavese, M. Mechanical Properties of Mortar Containing Waste Plastic (PVC) as Aggregate Partial Replacement. *Case Stud. Constr. Mater.* **2020**, *13*, No. e00467.
(8) Manjunatha, M.; Seth, D.; Kvgd, B.; A, B. Engineering Properties and Environmental Impact Assessment of Green Concrete Prepared with PVC Waste Powder: A Step towards Sustainable Approach. *Case Stud. Constr. Mater.* **2022**, *17*, No. e01404.
(9) Qiao, W. M.; Song, Y.; Yoon, S. H.; Korai, Y.; Mochida, I.; Katou, O. Preparation of PVC Pitch from Waste Pipe. *Carbon N. Y.* **2005**, *43*, 2022−2025.
(10) Eryildiz, B.; Ozbey-Unal, B.; Gezmis-Yavuz, E.; Koseoglu-Imer, D. Y.; Keskinler, B.; Koyuncu, I. Flux-Enhanced Reduced Graphene Oxide (RGO)/PVDF Nanofibrous Membrane Distillation Membranes for the Removal of Boron from Geothermal Water. *Sep. Purif. Technol.* **2021**, *274*, No. 119058.
(11) Zhao, J.; Zhang, J.; Zhou, T.; Liu, X.; Yuan, Q.; Zhang, A. New Understanding on the Reaction Pathways of the Polyacrylonitrile Copolymer Fiber Pre-Oxidation: Online Tracking by Two-Dimensional Correlation FTIR Spectroscopy. *RSC Adv.* **2016**, *6*, 4397−4409.
(12) Chen, Y.; Wang, N.; Jensen, M.; Li, X. Low-Temperature Welded PAN/TPU Composite Nanofiber Membranes for Water Filtration. *J. Water Process Eng.* **2022**, *47*, No. 102806.
(13) Li, H.; Mu, P.; Li, J.; Wang, Q. Inverse Desert Beetle-like ZIF-8/PAN Composite Nanofibrous Membrane for Highly Efficient Separation of Oil-in-Water Emulsions. *J. Mater. Chem. A* **2021**, *9*, 4167−4175.
(14) Wu, M.; Liu, W.; Mu, P.; Wang, Q.; Li, J. Sacrifice Template Strategy to the Fabrication of a Self-Cleaning Nanofibrous Membrane for Efficient Crude Oil-in-Water Emulsion Separation with High Flux. *ACS Appl. Mater. Interfaces* **2020**, *12*, 53484−53493.
(15) Wang, L.; Ali, J.; Zhang, C.; Mailhot, G.; Pan, G. Simultaneously Enhanced Photocatalytic and Antibacterial Activities of TiO2/Ag Composite Nanofibers for Wastewater Purification. *J. Environ. Chem. Eng.* **2020**, *8*, 102104.
(16) Kanjwal, M. A.; Alm, M.; Thomsen, P.; Barakat, N. A. M.; Chronakis, I. S. Hybrid Matrices of TiO2 and TiO2−Ag Nanofibers with Silicone for High Water Flux Photocatalytic Degradation of Dairy Effluent. *J. Ind. Eng. Chem.* **2016**, *33*, 142−149.
(17) Zulfi, A.; Hapidin, D. A.; Munir, M. M.; Iskandar, F.; Khairurrijal, K. The Synthesis of Nanofiber Membranes from Acrylonitrile Butadiene Styrene (ABS) Waste Using Electrospinning for Use as Air Filtration Media. *RSC Adv.* **2019**, *9*, 30741−30751.
(18) Huang, Z. M.; Zhang, Y. Z.; Kotaki, M.; Ramakrishna, S. A Review on Polymer Nanofibers by Electrospinning and Their Applications in Nanocomposites. *Compos. Sci. Technol.* **2003**, *63*, 2223−2253.
(19) Zulfi, A.; Munir, M. M.; Hapidin, D. A.; Rajak, A.; Edikresnha, D.; Iskandar, F.; Khairurrijal, K. Air Filtration Media from Electrospun Waste High-Impact Polystyrene Fiber Membrane. *Mater. Res. Express* **2018**, *5*, 3.
(20) Musa, I.; Raffin, G.; Hangouet, M.; Martin, M.; Bausells, J.; Zine, N.; Bellagambi, F.; Jaffrezic-renault, N.; Errachid, A. Electrospun PVC-Nickel Phthalocyanine Composite Nanofiber Based Conductometric Methanol Microsensor. *Microchem. J.* **2022**, *182*, No. 107899.
(21) Zhang, T.; Nazarov, R.; Pham, L. Q.; Soboleva, V.; Demchenko, P.; Uspenskaya, M.; Olekhnovich, R.; Khodzitsky, M. Polymer Composites Based on Polyvinyl Chloride Nanofibers and Polypropylene Films for Terahertz Photonics. *Opt. Mater. Express* **2020**, *10*, 2456.
(22) Hezarjaribi, M.; Bakeri, G.; Sillanpää, M.; Chaichi, M. J.; Akbari, S.; Rahimpour, A. Novel Adsorptive PVC Nanofibrous/Thiol-Functionalized TNT Composite UF Membranes for Effective Dynamic Removal of Heavy Metal Ions. *J. Environ. Manage.* **2021**, *284*, No. 111996.
(23) Pascariu, P.; Cojocaru, C.; Airinei, A.; Olaru, N.; Rosca, I.; Koudoumas, E.; Suchea, M. P. Innovative Ag−TiO2 Nanofibers with Excellent Photocatalytic and Antibacterial Actions. *Catalysts* **2021**, *11*, 1234.
(24) Batool, Z.; Raffi, M.; Zakria, M.; Shakoor, R. I.; Rashid, R.; Mehmood, M.; Mirza, M. A. Effect of Ag Loading on the Microstructure of TiO2 Electrospun Nanofibers. *J. Cluster Sci.* **2017**, *28*, 1857−1870.
(25) Ji, L.; Qin, X.; Zheng, J.; Zhou, S.; Xu, T.; Shi, G. Synthesis of Ag−Carbon−TiO2 Composite Tubes and Their Antibacterial and Organic Degradation Properties. *J. Sol-Gel Sci. Technol.* **2020**, *93*, 291−301.
(26) Hartati, S.; Zulfi, A.; Maulida, P. Y. D.; Yudhowijoyo, A.; Dioktyanto, M.; Saputro, K. E.; Noviyanto, A.; Rochman, N. T. Synthesis of Electrospun PAN/TiO2/Ag Nanofibers Membrane As Potential Air Filtration Media with Photocatalytic Activity. *ACS Omega* **2022**, *7*, 10516−10525.
(27) Zhang, Y.; Li, J.; Li, W.; Kang, D. Synthesis of One-Dimensional Mesoporous Ag Nanoparticles-Modified TiO2 Nanofibers by Electrospinning for Lithium Ion Batteries. *Materials* **2019**, *12*, 2630.
(28) Park, J. Y.; Hwang, K. J.; Lee, J. W.; Lee, I. H. Fabrication and Characterization of Electrospun Ag Doped TiO2 Nanofibers for Photocatalytic Reaction. *J. Mater. Sci.* **2011**, *46*, 7240−7246.
(29) Dakhel, A. A. Critical Role of Hydrogenation for Creation of Magnetic Cd−Cu Co-Incorporated TiO2 Nanocrystallites. *Appl. Phys. A: Mater. Sci. Process.* **2019**, *126*, 1−8.
(30) Liu, L.; Son, M.; Chakraborty, S.; Bhattacharjee, C.; Choi, H. Fabrication of Ultra-Thin Polyelectrolyte/Carbon Nanotube Membrane by Spray-Assisted Layer-by-Layer Technique: Characterization and Its Anti-Protein Fouling Properties for Water Treatment. *Desalin. Water Treat.* **2013**, *51*, 6194−6200.
(31) Constantinescu, B.; Bugoi, R.; Oberlander-Tarnoveanu, E.; Parvan, K. Some Considerations on X-Ray Fluorescence Use in Museum Measurements - the Case of Medieval Silver Coins. *Rom. Reports Phys.* **2005**, *57*, 1021−1031.
(32) Ferretti, M. The Investigation of Ancient Metal Artefacts by Portable X-Ray Fluorescence Devices. *J. Anal. At. Spectrom.* **2014**, *29*, 1753−1766.
(33) Iranizadeh, S. T.; Pourafshari Chenar, M.; Mahboub, M. N.; Namaghi, H. A. PREPARATION AND CHARACTERIZATION OF THIN-FILM COMPOSITE REVERSE OSMOSIS MEMBRANE

https://doi.org/10.1021/acsomega.3c01632
ACS Omega 2023, 8, 23622−23632

ON A NOVEL AMINOSILANE-MODIFIED POLYVINYL CHLORIDE SUPPORT. *Brazilian J. Chem. Eng.* **2019**, *36*, 251−264.
(34) Lyu, Y.; Yin, H.; Chen, Y.; Zhang, Q.; Shi, X. Structure and Evolution of Multiphase Composites for 3D Printing. *J. Mater. Sci.* **2020**, *55*, 6861−6874.
(35) Lubasova, D.; Barbora, S. Antibacterial Efficiency of Nanofiber Membranes with Biologically Active Nanoparticles. *Int. Conf. Agric.* **2014**, 55.
(36) El Sayed, A. M.; Morsi, W. M. Dielectric Relaxation and Optical Properties of Polyvinyl Chloride/Lead Monoxide Nanocomposites. *Polym. Compos.* **2013**, *34*, 2031−2039.
(37) Abdel-Baset, T.; Elzayat, M.; Mahrous, S. Characterization and Optical and Dielectric Properties of Polyvinyl Chloride/Silica Nanocomposites Films. *Int. J. Polym. Sci.* **2016**, *2016*, 1.
(38) Rahma, A.; Munir, M. M.; Khairurrijal; Prasetyo, A.; Suendo, V.; Rachmawati, H. Intermolecular Interactions and the Release Pattern of Electrospun Curcumin-Polyvinyl(Pyrrolidone) Fiber. *Biol. Pharm. Bull.* **2016**, *39*, 163−173.
(39) El-Desoky, M. M.; Morad, I.; Wasfy, M. H.; Mansour, A. F. Synthesis, Structural and Electrical Properties of PVA/TiO2 Nanocomposite Films with Different TiO2 Phases Prepared by Sol−Gel Technique. *J. Mater. Sci.: Mater. Electron.* **2020**, *31*, 17574−17584.
(40) Desiati, R. D.; Taspika, M.; Sugiarti, E.; Desiati, R. D.; Taspika, M.; Sugiarti, E. Effect of Calcination Temperature on the Antibacterial Activity of TiO2/Ag Nanocomposite. *MRE* **2019**, *6*, No. 095059.
(41) Duan, Z.; Huang, Y.; Zhang, D.; Chen, S. Electrospinning Fabricating Au/TiO2 Network-like Nanofibers as Visible Light Activated Photocatalyst. *Sci. Rep.* **2019**, *9*, 1−9.
(42) Luttrell, T.; Halpegamage, S.; Tao, J.; Kramer, A.; Sutter, E.; Batzill, M. Why Is Anatase a Better Photocatalyst than Rutile? - Model Studies on Epitaxial TiO2 Films. *Sci. Rep.* **2014**, *4*, 4043.
(43) Meng, Y. A Sustainable Approach to Fabricating Ag Nanoparticles/PVA Hybrid Nanofiber and Its Catalytic Activity. *Nanomaterials* **2015**, *5*, 1124−1135.
(44) Mosquera, A.; National, S.; Albella, J. M.; National, S.; Navarro, V.; Endrino, J. L. Effect of Silver on the Phase Transition and Wettability of Titanium Oxide Films. *Sci. Rep.* **2016**, 32171.
(45) Pham, L. Q.; Solovieva, A. Y.; Uspenskaya, M. V.; Olekhnovich, R. O.; Sitnikova, V. E.; Strelnikova, I. E.; Kunakova, A. M. High-Porosity Polymer Composite for Removing Oil Spills in Cold Regions. *ACS Omega* **2021**, *6*, 20512−20521.
(46) Ramesh, S.; Leen, K. H.; Kumutha, K.; Arof, A. K. FTIR Studies of PVC/PMMA Blend Based Polymer Electrolytes. *Spectrochim. Acta Part A Mol. Biomol. Spectrosc.* **2007**, *66*, 1237−1242.
(47) Kunnamareddy, M.; Diravidamani, B.; Rajendran, R.; Singaram, B.; Varadharajan, K. Synthesis of Silver and Sulphur Codoped TiO2 Nanoparticles for Photocatalytic Degradation of Methylene Blue. *J. Mater. Sci.: Mater. Electron.* **2018**, *29*, 18111−18119.
(48) Norouzi, M.; Fazeli, A.; Tavakoli, O. Phenol Contaminated Water Treatment by Photocatalytic Degradation on Electrospun Ag/TiO2 Nanofibers: Optimization by the Response Surface Method. *J. Water Process Eng.* **2020**, *37*, No. 101489.
(49) Zulfi, A.; Hapidin, D. A.; Saputra, C.; Mustika, W. S.; Munir, M. M.; Khairurrijal, K. The Synthesis of Fiber Membranes from High-Impact Polystyrene (HIPS) Waste Using Needleless Electrospinning as Air Filtration Media. *Mater. Today Proc.* **2019**, *13*, 154−159.
(50) Verbovy, D. M.; Smagala, T. G.; Brynda, M. A.; Fawcett, W. R. A FTIR Study of Ion-Solvent Interactions in N,N-Dimethylacetamide. *J. Mol. Liq.* **2006**, *129*, 13−17.
(51) Watanabe, T.; Nakajima, A.; Wang, R.; Minabe, M.; Koizumi, S.; Fujishima, A.; Hashimoto, K. Photocatalytic Activity and Photoinduced Hydrophilicity of Titanium Dioxide Coated Glass. *Thin Solid Films* **1999**, *351*, 260−263.
(52) Tamaki, Y.; Furube, A.; Murai, M.; Hara, K.; Katoh, R.; Tachiya, M. Direct Observation of Reactive Trapped Holes in TiO2 Undergoing Photocatalytic Oxidation of Adsorbed Alcohols: Evaluation of the Reaction Rates and Yields. *J. Am. Chem. Soc.* **2006**, *128*, 416−417.
(53) Kudhier, M. A.; Alkareem, R. A. S. A.; Sabry, R. S. Enhanced Photocatalytic Activity of TiO2-CdS Composite Nanofibers under Sunlight Irradiation. *J. Mech. Behav. Mater.* **2021**, *30*, 213−219.
(54) Kim, K. D.; Han, D. N.; Lee, J. B.; Kim, H. T. Formation and Characterization of Ag-Deposited TiO2 Nanoparticles by Chemical Reduction Method. *Scr. Mater.* **2006**, *54*, 143−146.
(55) Seery, M. K.; George, R.; Floris, P.; Pillai, S. C. Silver Doped Titanium Dioxide Nanomaterials for Enhanced Visible Light Photocatalysis. *J. Photochem. Photobiol., A* **2007**, *189*, 258−263.
(56) Ren, H. T.; Han, J.; Li, T. T.; Liang, Y.; Jing, M. Z.; Jiang, S. M.; Lin, J. H.; Lou, C. W. Facile Preparation of PAN@Ag−Ag2O/TiO2 Nanofibers with Enhanced Photocatalytic Activity and Reusability toward Oxidation of As(III). *J. Mater. Sci.* **2020**, *55*, 11310−11324.
(57) Fauzi, A.; Hapidin, D. A.; Munir, M. M.; Iskandar, F.; Khairurrijal, K. A Superhydrophilic Bilayer Structure of a Nylon 6 Nanofiber/Cellulose Membrane and Its Characterization as Potential Water Filtration Media. *RSC Adv.* **2020**, *10*, 17205−17216.
(58) Sawitri, A.; Munir, M. M.; Edikresnha, D.; Sandi, A.; Fauzi, A.; Rajak, A.; Natalia, D.; Khairurrijal, K. An Investigation on Bilayer Structures of Electrospun Polyacrylonitrile Nanofibrous Membrane and Cellulose Membrane Used as Filtration Media for Apple Juice Clarification. *Mater. Res. Express* **2018**, *5*, 54003.
(59) Liu, Y.; Wang, R.; Ma, H.; Hsiao, B. S.; Chu, B. High-Flux Microfiltration Filters Based on Electrospun Polyvinylalcohol Nanofibrous Membranes. *Polymer (Guildf).* **2013**, *54*, 548−556.
(60) Wang, R.; Liu, Y.; Li, B.; Hsiao, B. S.; Chu, B. Electrospun Nanofibrous Membranes for High Flux Microfiltration. *J. Membr. Sci.* **2012**, *392*−*393*, 167−174.
(61) Liu, H. R.; Raza, A.; Aili, A.; Lu, J. Y.; Alghaferi, A.; Zhang, T. J. Sunlight-Sensitive Anti-Fouling Nanostructured TiO2 Coated Cu Meshes for Ultrafast Oily Water Treatment. *Sci. Rep.* **2016**, *6*, 1−10.
(62) Asmatulu, R.; Muppalla, H.; Veisi, Z.; Khan, W. S.; Asaduzzaman, A.; Nuraje, N. Study of Hydrophilic Electrospun Nanofiber Membranes for Filtration of Micro and Nanosize Suspended Particles. *Membranes* **2013**, *3*, 375−388.
(63) Gopal, R.; Kaur, S.; Ma, Z.; Chan, C.; Ramakrishna, S.; Matsuura, T. Electrospun Nanofibrous Filtration Membrane. *J. Membr. Sci.* **2006**, *281*, 581−586.
(64) Seyed Shahabadi, S. M.; Mousavi, S. A.; Bastani, D. High Flux Electrospun Nanofiberous Membrane: Preparation by Statistical Approach, Characterization, and Microfiltration Assessment. *J. Taiwan Inst. Chem. Eng.* **2016**, *59*, 474−483.
(65) Nur'aini, S.; Zulfi, A.; Bagas, B.; Arrosyid, H.; Rafryanto, A. F.; Noviyanto, A.; Dian, A.; Hapidin, A.; Feriyanto, D.; Kurniawan, C.; Saputro, E.; Khairurrijal, K.; Rochman, N. T. Waste Acrylonitrile Butadiene Styrene (ABS) Incorporated with Polyvinylpyrrolidone (PVP) for Potential Water Filtration Membrane. *RSC Adv.* **2022**, DOI: 10.1039/d2ra05969j.
(66) Jamil, T.; Munir, S.; Wali, Q.; Shah, G. J.; Khan, M. E.; Jose, R. Water Puri Fi Cation through a Novel Electrospun Carbon Nano Fi Ber Membrane. 2021, *6*, 1−34751, DOI: 10.1021/acsomega.1c05197.
(67) Wang, Z.; Sahadevan, R.; Crandall, C.; Menkhaus, T. J.; Fong, H. Hot-Pressed PAN / PVDF Hybrid Electrospun Nanofiber Membranes for Ultrafiltration. *J. Membr. Sci.* **2020**, *611*, No. 118327.
(68) Hassan, M. L.; Fadel, S. M.; Abouzeid, R. E.; Elseoud, W. S. A. Water Purification Ultrafiltration Membranes Using Nanofibers from Unbleached and Bleached Rice Straw. *Sci. Rep.* **2020**, 1−9.
(69) Goetz, L. A.; Jalvo, B.; Rosal, R.; Mathew, A. P. Superhydrophilic Anti-Fouling Electrospun Cellulose Acetate Membranes Coated with Chitin Nanocrystals for Water Filtration. *J. Membr. Sci.* **2016**, *510*, 238−248.
(70) Du, X.; Zheng, H.; Zhang, Y.; Zhao, N.; Chen, M. Journal of the Taiwan Institute of Chemical Engineers Pore Structure Design and Optimization of Electrospun PMIA Nanofiber Membrane. *J. Taiwan Inst. Chem. Eng.* **2022**, *139*, No. 104512.
(71) Arribas, P.; García-payo, M. C.; Khayet, M.; Gil, L. Heat-Treated Optimized Polysulfone Electrospun Nanofibrous Membranes

for High Performance Wastewater Microfiltration. *Sep. Purif. Technol.* **2018**, *2019*, 323−336.
(72) Arahman, N.; Jakfar, J.; Dzulhijjah, W. A.; Halimah, N.; Silmina, S.; Aulia, M. P.; Fahrina, A.; Bilad, M. R. Hydrophilic Antimicrobial Polyethersulfone Membrane for Removal of Turbidity of Well-Water. *Water* **2022**, 3769.
(73) Karimi, E.; Raisi, A.; Aroujalian, A. TiO 2 -Induced Photo-Cross-Linked Electrospun Polyvinyl Alcohol Nano Fi Bers Micro Fi Ltration. *Membranes.* **2016**, *99*, 642−653.
(74) Yadav, G. M. P.; Rao, G. L.; Madduleti, M.; Raghavendra, H.; Kumar, P. A.; Kumar, N. S.; Vijeyudu, K.; Reddy, M. S. An Experimental Analysis on the Effect of Filler Material (CaCo 3) On PVC Pipes. 2015, 3 (2), 48−55.
(75) Prahasti, G.; Zulfi, A.; Khairurrijal, K. Synthesis of Fiber Membranes from Polyvinyl Alcohol (PVA)/Shell Extract of Melinjo (SEM) Using Electrospinning Method. *Mater. Today Proc.* **2021**, *44*, 3400−3402.

https://doi.org/10.1021/acsomega.3c01632
ACS Omega 2023, 8, 23622−23632